Strain and Composition Engineering of Excited-state Carrier Recombination Dynamics in GaAs/GaP and GaAs/AlAs Superlattices: Insights from Time-Domain Nonadiabatic Molecular Dynamics Simulations

Yue Tang [a], Yipeng Wang [b], Hong Zhang [c], Pengfei Lu [d, *], and Xinlu Cheng [a, *]

[a] Institute of Atomic and Molecular Physics, Sichuan University, Chengdu 610065, China

[b] College of Applied Technology, Shenzhen University, Shenzhen 518061, China

[c] College of Physics, Sichuan University, Chengdu 610064, China.

[d] State Key Laboratory of Information Photonics and Optical Communications and School of Electronic Engineering, Beijing University of Posts and Telecommunications, Beijing 100876, China.

List of Figures

Note 1 Elastic constants of GaAs/GaP and GaAs/AlAs superlattices.

GaAs/GaP and GaAs/AlAs exhibit identical forms of the elastic matrix:

$$C_{\text{superlattice}} = \begin{pmatrix} C_{11} & C_{12} & C_{13} & & & \\ . & C_{11} & C_{13} & & & \\ . & . & C_{33} & & & \\ & & & C_{44} & & \\ & & & & C_{44} & \\ & & & & & C_{66} \end{pmatrix}$$

Elastic constants (GPa) of GaAs/GaP are as follows:

$$C_{\text{GaAs/GaP}} = \begin{pmatrix} 107.3366 & 46.2395 & 43.4099 & & & \\ . & 107.3366 & 43.4099 & & & \\ . & . & 106.8399 & & & \\ & & & 55.7396 & & \\ & & & & 55.7396 & \\ & & & & & 56.0052 \end{pmatrix}$$

Elastic constants (GPa) of GaAs/AlAs are as follows:

$$C_{\text{GaAs/AlAs}} = \begin{pmatrix} 101.9251 & 46.0447 & 46.2020 & & & \\ . & 101.9251 & 46.2020 & & & \\ . & . & 101.7941 & & & \\ & & & 50.7471 & & \\ & & & & 50.7471 & \\ & & & & & 50.9357 \end{pmatrix}$$

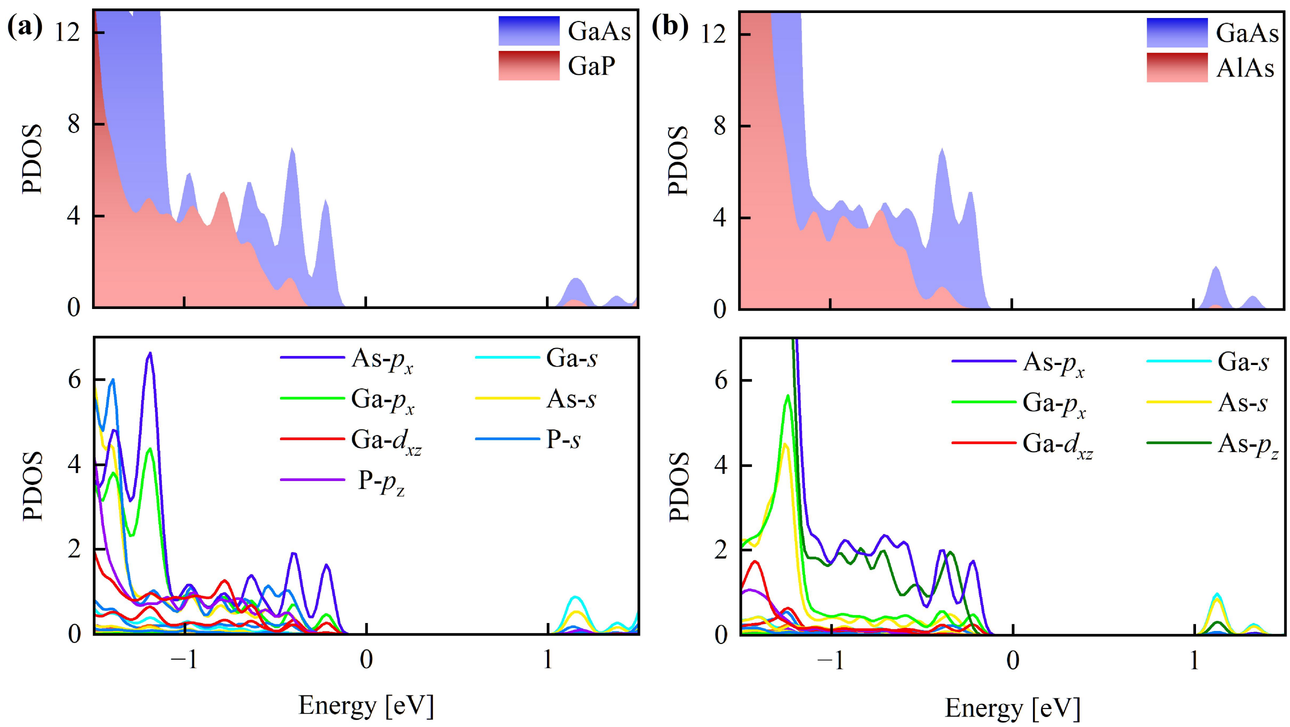

Fig. S1 Projected density of states of (a) GaAs/GaP and (b) GaAs/AlAs superlattices.

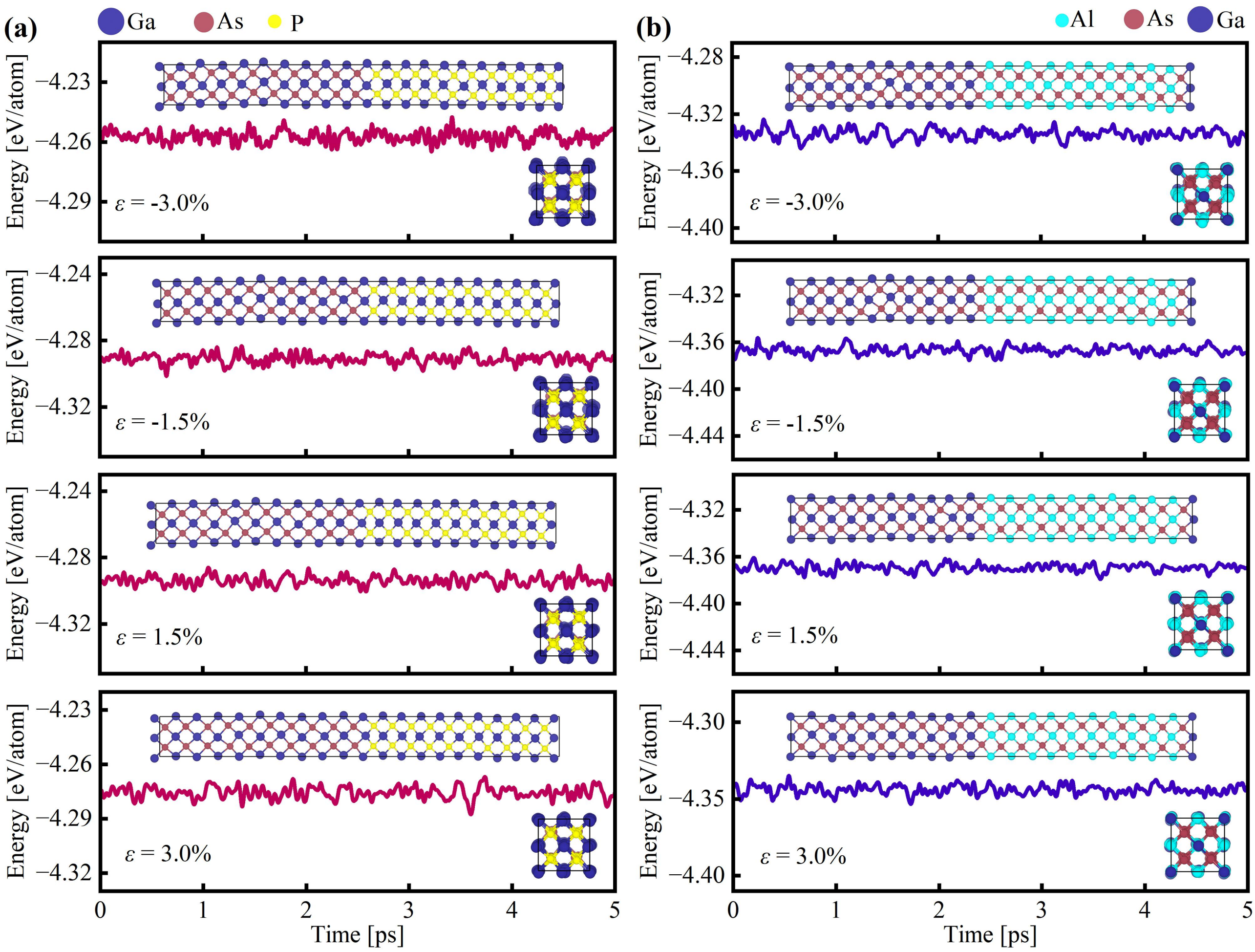

Fig. S2 AIMD results of strained (a) GaAs/GaP and (b) GaAs/AlAs at 300 K. Insets are side and top views of the structures after simulations.

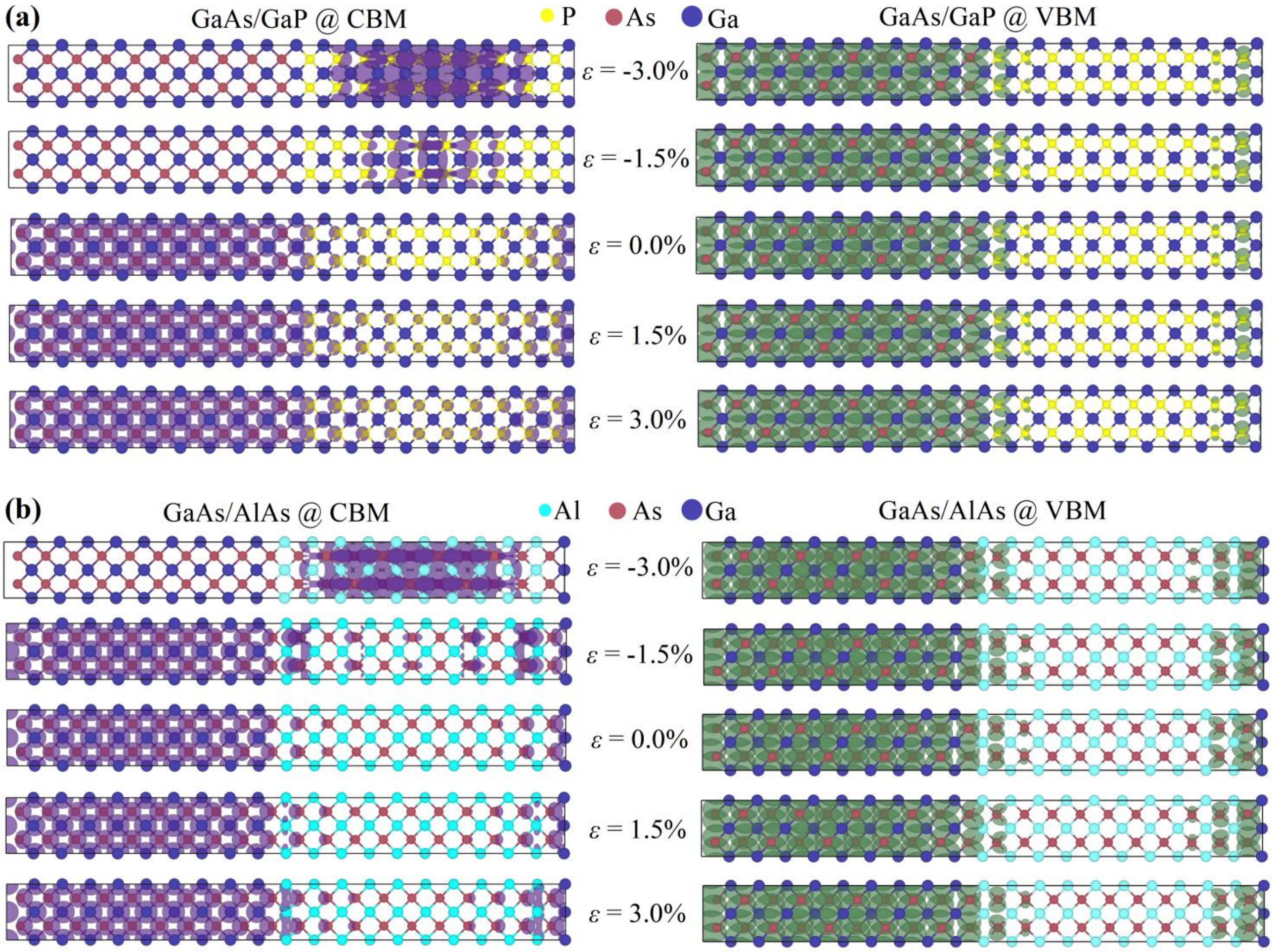

Fig. S3 Orbital distribution of the CBM and VBM for (a) GaAs/GaP and (b) GaAs/AlAs under various strains.

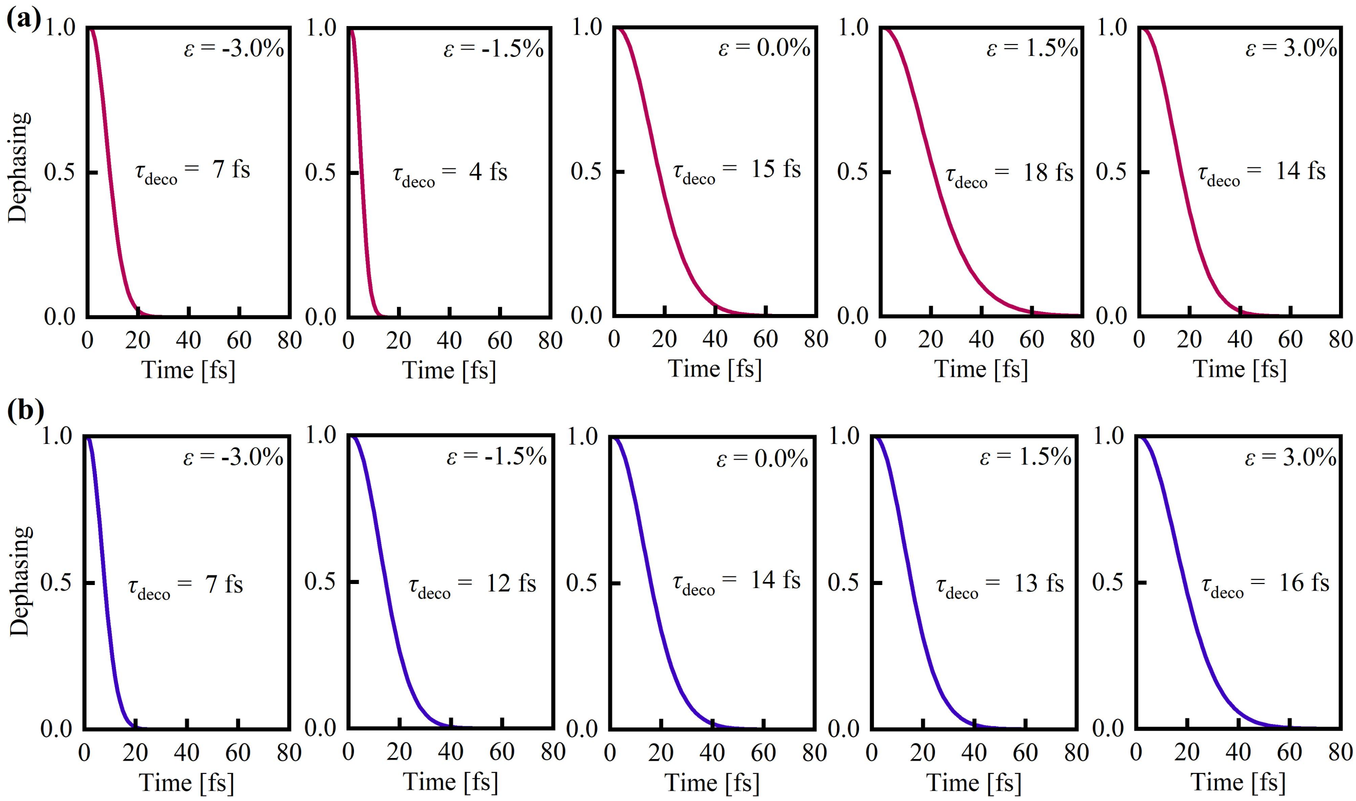

Fig. S4 Dephasing function of (a) GaAs/GaP and (b) GaAs/AlAs under different strains, with the fitted decoherence times.

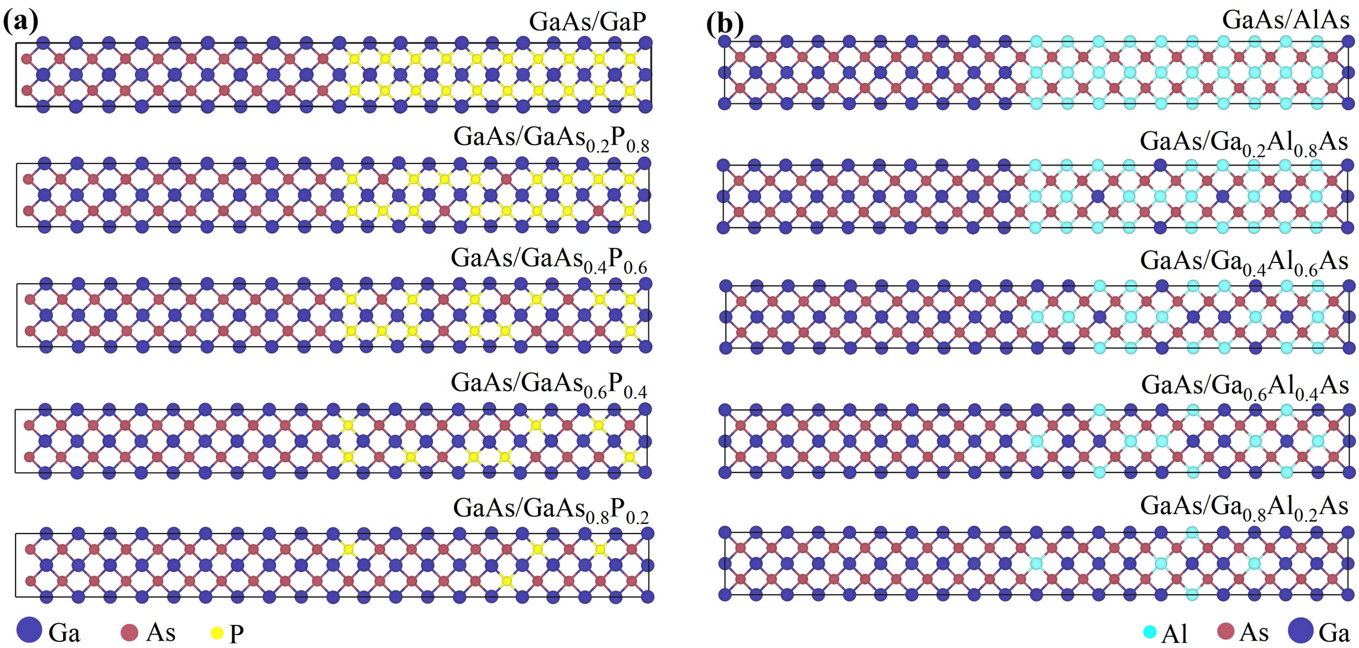

Fig. S5 Optimized structures of (a) GaAs/GaAs$_x$P$_{1-x}$ and (b) GaAs/Ga$_x$Al$_{1-x}$As superlattices.

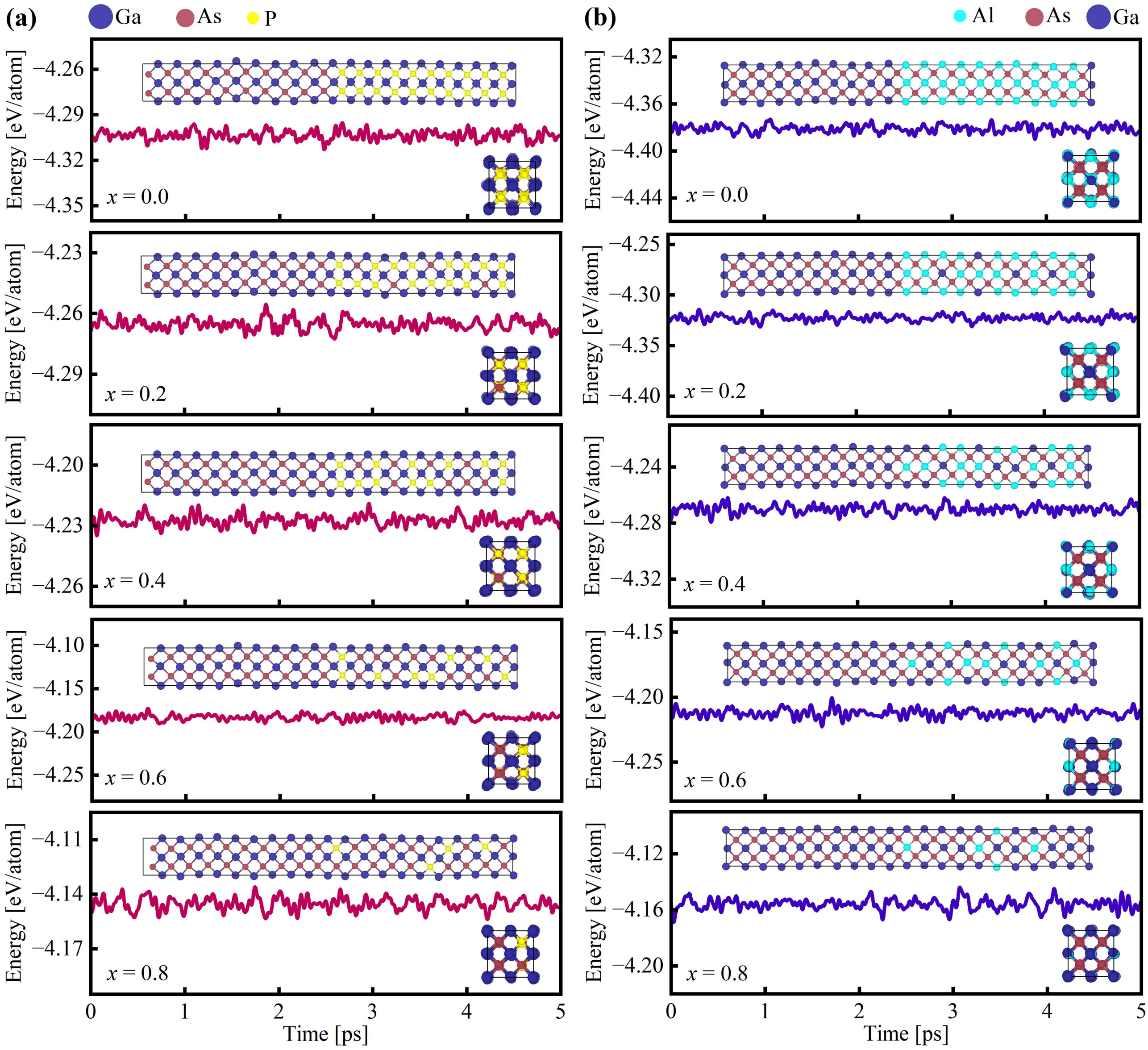

Fig. S6 AIMD results of (a) GaAs/GaAs$_x$P$_{1-x}$ and (b) GaAs/Ga$_x$Al$_{1-x}$As at 300 K. Insets are side and top views of the structures after simulations.

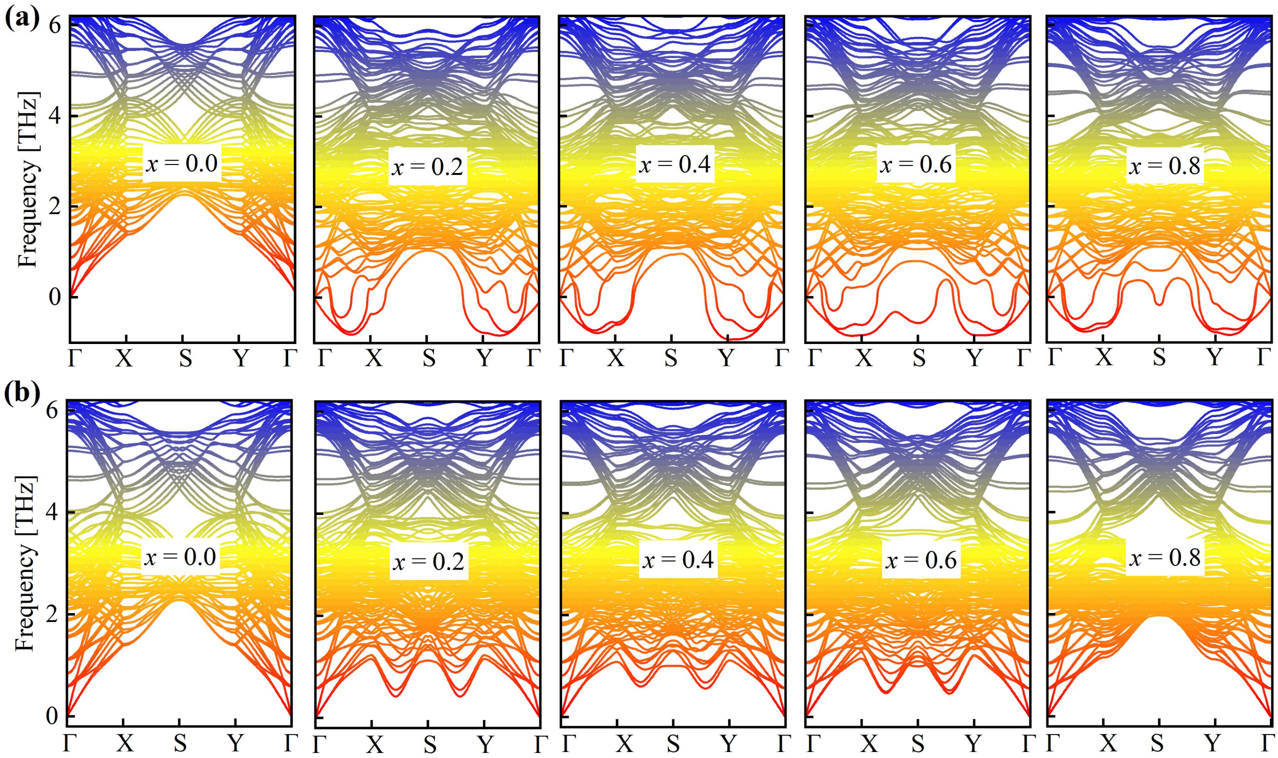

Fig. S7 Phonon dispersion spectra of (a) GaAs/GaAs$_x$P$_{1-x}$ and (b) GaAs/Ga$_x$Al$_{1-x}$As.

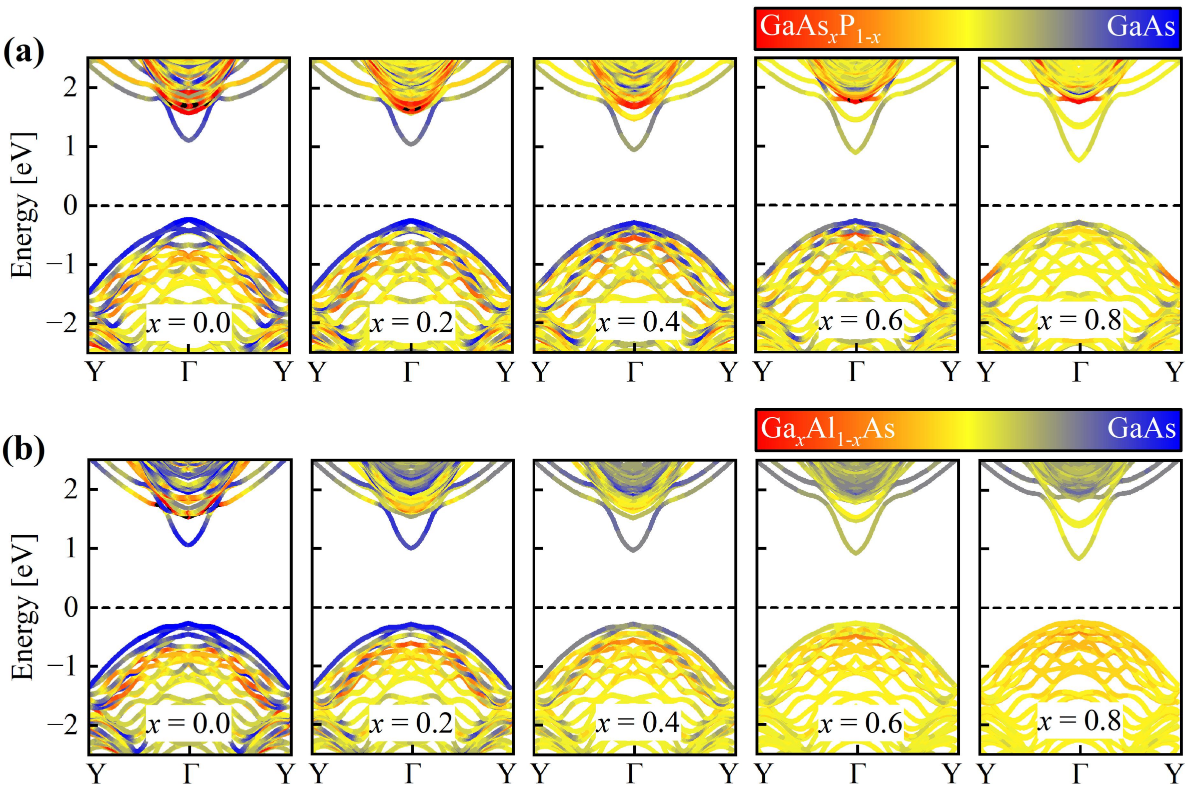

Fig. S8 Projected band structures of (a) GaAs/GaAs$_x$P$_{1-x}$ and (b) GaAs/Ga$_x$Al$_{1-x}$As with the HSE06 method. Dashed lines represent the Fermi levels.

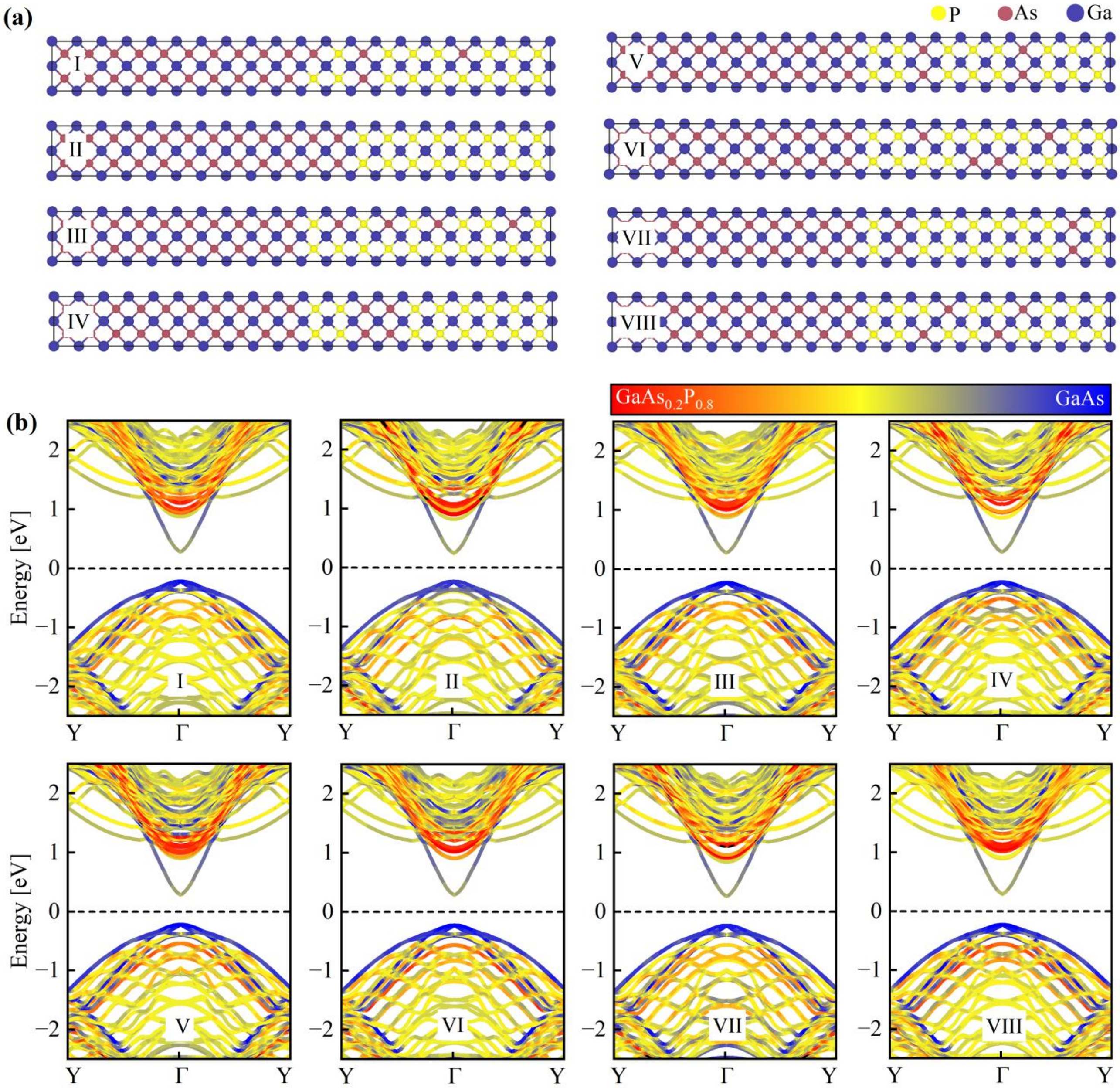

Fig. S9 (a) Optimized structures and (b) projected band structures for different configurations of $GaAs/GaAs_{0.2}P_{0.8}$. Dashed lines represent the Fermi levels.

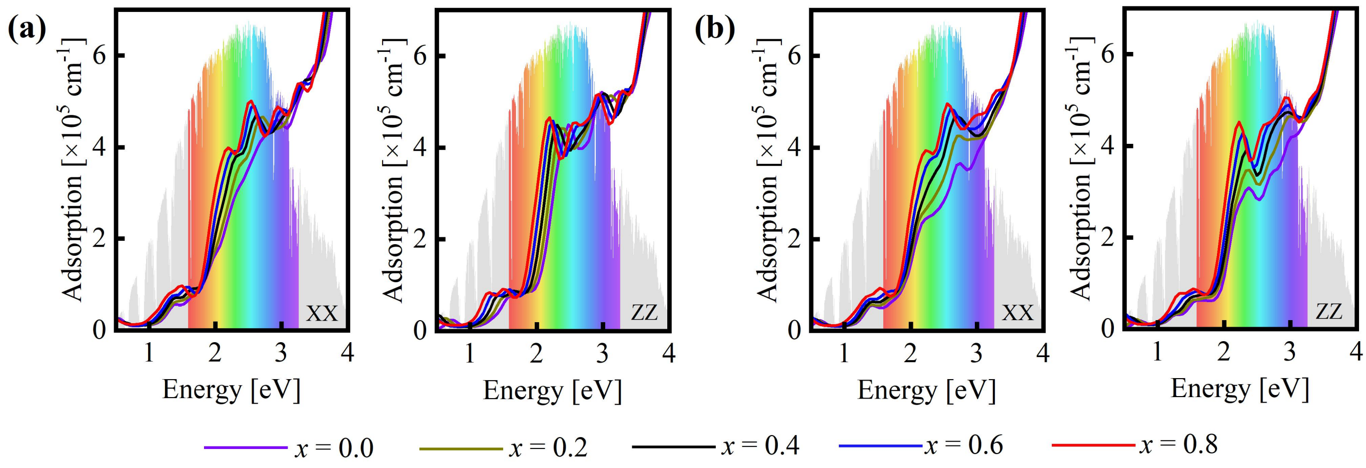

Fig. S10 Light absorption spectra of (a) GaAs/GaAs$_x$P$_{1-x}$ and (b) GaAs/Ga$_x$Al$_{1-x}$As along the XX and ZZ directions.

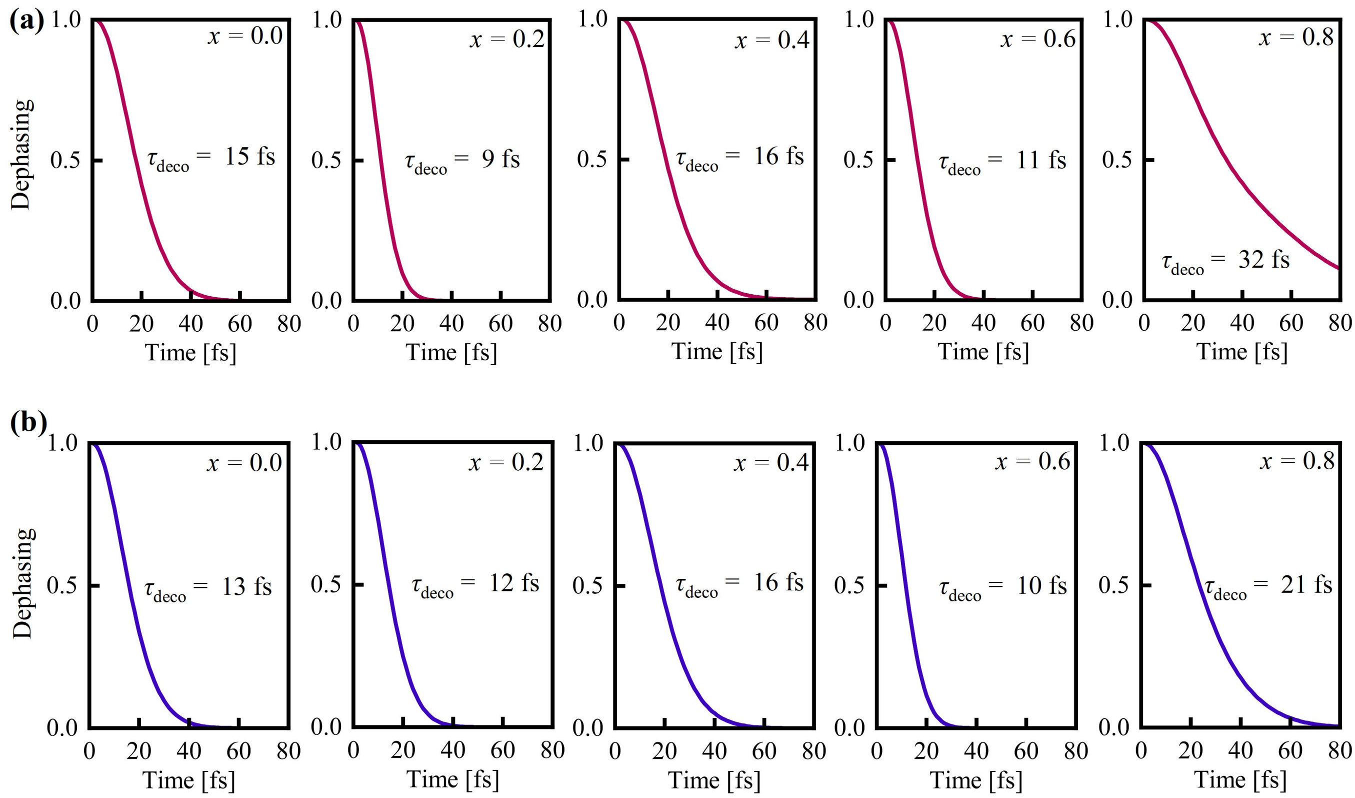

Fig. S11 Dephasing function of (a) GaAs/GaAs$_x$P$_{1-x}$ and (b) GaAs/Ga$_x$Al$_{1-x}$As, with the fitted decoherence times.

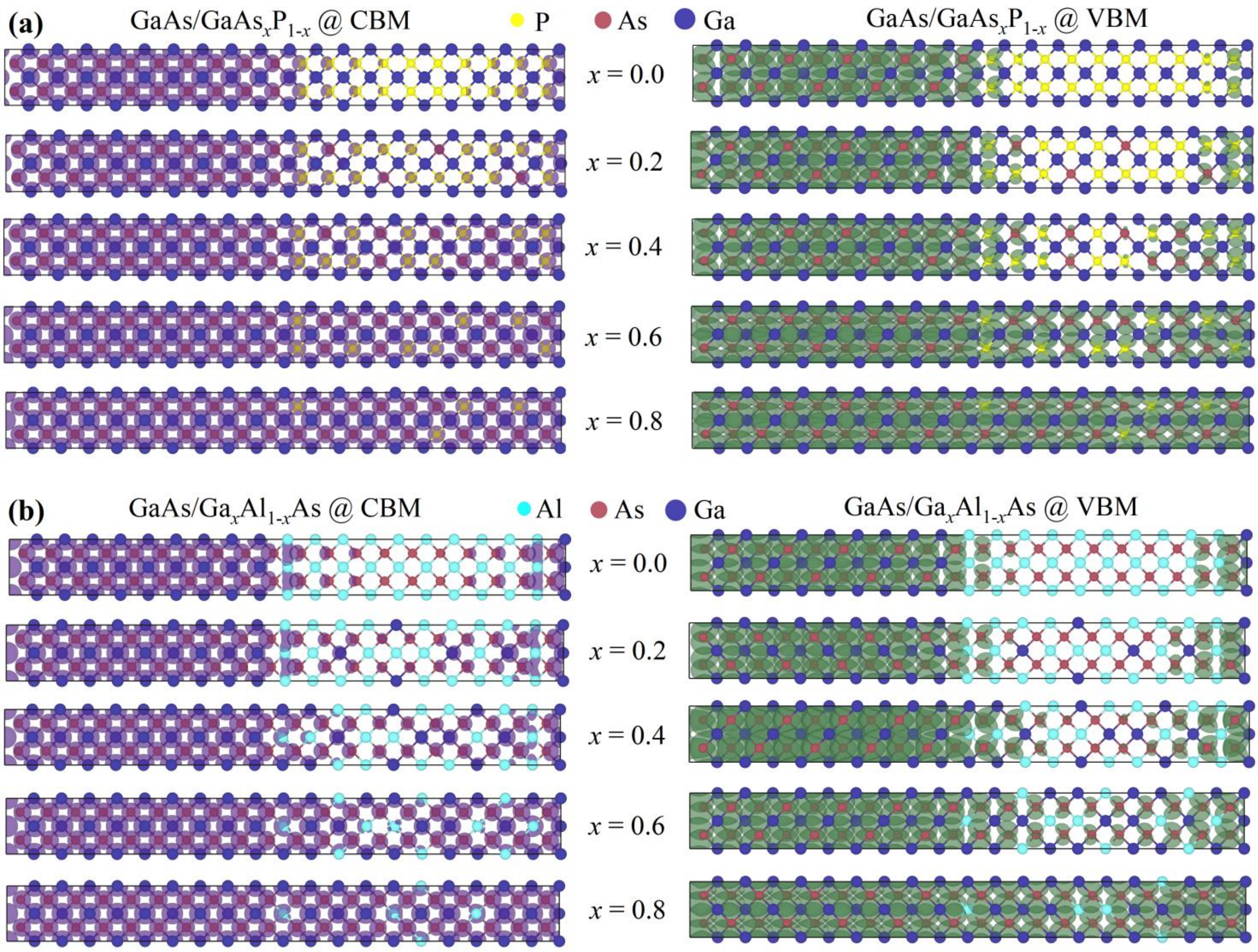

Fig. S12 Orbital distribution of the CBM and VBM for (a) GaAs/GaAs$_x$P$_{1-x}$ and (b) GaAs/Ga$_x$Al$_{1-x}$As.

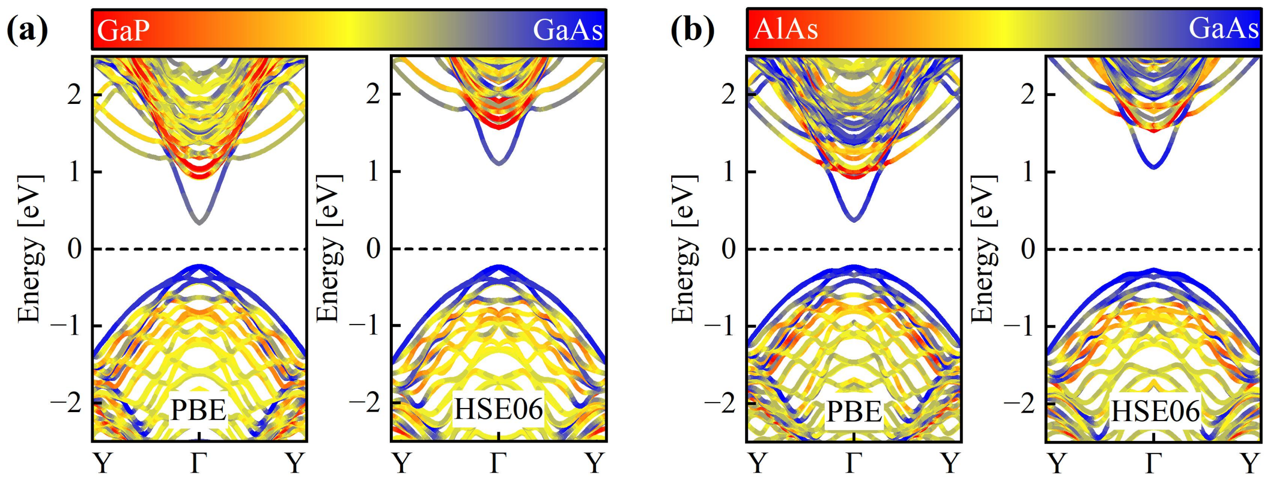

Fig. S13 Projected band structures of (a) GaAs/GaP and (b) GaAs/AlAs with the PBE and HSE06 methods. Dashed lines represent the Fermi levels.